Contaminant Leaching from Saltstone

By

J.C. Seaman* and F.M. Coutelot**

*Senior Research Scientist
Assistant Director – Research/Quality Assurance
Savannah River Ecology Laboratory
The University of Georgia
Aiken, SC 29802
Phone: 803-725-0977
seaman@srel.uga.edu

**Assistant Research Scientist
coutelot@uga.edu

REVIEWS AND APPROVALS

Authors:

John C. Seaman, SREL Associate Director-Research
Senior Research Scientist — Date: 9/29/17

Review:

Larry Bryan, SREL Research Associate — Date: 9.29.2017

Approval:

Steven Simner, CTF Savannah River Remediation LLC — Date: 10/2/2017

Table of Contents

1.0 Executive Summary

At the Department of Energy's Savannah River Site (SRS) chemically reducing materials, such as blast furnace slag (BFS), are added to grout formulations mixed with low-level radioactive salt waste solutions in order to enhance the attenuation of redox sensitive contaminants (e.g., technetium-99 (^{99}Tc)). The resulting cementitious material, known as *saltstone*, is deposited in a series of concrete vaults for long-term disposal at the Saltstone Disposal Facility (SDF). Such chemically reducing grouts provide both a physical (i.e., low saturated hydraulic conductivities (SHC) that limit H_2O turnover and O_2 exposure) and a chemical barrier (i.e., residual reductive capacity) to contaminant release. However, many of the previous experiments evaluating the ability of saltstone to chemically reduce and immobilize Tc and retain other radioactive contaminants, such as iodine-129 (^{129}I), have been conducted using ground saltstone materials as sorbents. This practice is likely to reduce the moisture level in the material, expose new reactive surfaces and soluble constituents, enhance exposure to O_2 that may facilitate changes in redox status and alter sorbent properties in an unpredictable manner. Therefore, the current objective was to continue the development and testing of methods for evaluating contaminant partitioning within intact monolithic materials.

The current report contains data for both ^{99}Tc and ^{129}I from two related studies. Technetium-99 and ^{129}I spiked saltstone simulants were produced utilizing SRR prescribed formulations and subjected to varying curing durations under controlled temperature and humidity conditions chosen to mimic curing conditions within Saltstone Disposal Unit (SDU) Cell 2B. The same grout simulants were compared to actual intact saltstone retrieved (cured in place for approximately 20 months) from SDF-SDU Cell 2A. Contaminant mass transfer rates for the ^{129}I spiked saltstone simulants and SDF saltstone samples were assessed using EPA Method 1315, *Mass Transfer Rates of Constituents in Monolithic or Compacted Granular Materials Using a Semi-Dynamic Tank Leaching Procedure*. Similar data for other SDF contaminants, i.e., cesium-137 (^{137}Cs), ^{99}Tc, and nitrate (NO_3^-) was reported previously (Seaman, 2016).

EPA Method 1315 was recently adopted for evaluating contaminant leaching from intact monolithic materials. Results from Method 1315 were compared to a novel test method under development at the Savannah River Ecology Laboratory (SREL) known as the Dynamic Leaching Method (DLM). In the DLM method a flexible-wall permeameter cell is used to achieve saturated leaching through intact grout monoliths under an elevated hydraulic gradient in an effort to evaluate the persistence of reductive capacity and subsequent changes in contaminant partitioning that occur within intact saltstone monoliths. The composition of the chemical leachates from both tests can then be analyzed in an effort to identify critical reactions and solid phases controlling contaminant partitioning through geochemical modeling.

For the EPA 1315 tests the rate (μg cm^{-2} s^{-1}) of ^{129}I leaching from the SDF monoliths decreased over the course of the test, with the cumulative ^{129}I release histories initially conforming to diffusion controlled mechanisms for the purposes of data interpretation and comparison. The leaching rates for ^{129}I were similar to that of NO_3^-, as indicated by high effective diffusivities (D_e) and low leachability indices ($i.e.,\ LI = -\log[D_e]$). There was some variability in ^{129}I leaching rates between the three test

SDU-2A samples that was consistent with the pattern observed for ^{137}Cs. The variable rate of ^{137}Cs leaching presumably reflected differences in total ^{137}Cs present in the three SDU samples. For ^{129}I, the starting concentration of ^{129}I in the three test monoliths was based on the average value reported by SRNL for the characterization of the SDU-2A grout samples, i.e., 4.13 ± 0.88 pCi gm^{-1}.

For DLM testing, the current data set reflects the continued leaching of three test materials, a ^{99}Tc-spiked sample described in Seaman (2015) and two of the SDU-2A samples. The three samples were leached with an artificial groundwater (AGW) surrogate that was either degassed to remove O_2 or equilibrated with standard atmosphere. The K_{sat} values for the three samples varied greatly and made it difficult to control pore water residence times and maintain constant flow rates, complicating the interpretation of leaching data. In addition, the pH of samples was inconsistent with effluent ^{99}Tc levels if one assumed a reduced Tc precipitate (i.e., $TcO_2.2H_2O$ or $TcO_2.1.6H_2O$) controlled leaching behavior. To address this limitation, several different methods were evaluated for monitoring the effluent pH and oxidation reduction potential (ORP), including the testing of several commercially available flow-through sensors. However, flow-through sensors proved unreliable due to the low flow rates inherent to the DLM system, ranging from <0.1 to 2 mL d^{-1}, combined with the high alkalinity and salt content of the saltstone leachate. An alternate method was developed where a small volume of effluent could be sampled from within the tubing before it had reached the effluent collection vessel and then immediately monitored for pH and ORP. Effluent pH values for these samples were one to two pH units higher than effluent samples that were exposed to the atmosphere during extended sampling intervals. The ORP values for effluent samples were also lower as well, indicative of the lower redox conditions before the saltstone leachate was exposed to the atmosphere. Using the new sampling method, the effluent ^{99}Tc levels were generally consistent with the solubility for possible Tc(IV) solid phases, i.e., $TcO_2.2H_2O$ or $TcO_2.1.6H_2O$.

List of Figures

List of Tables

List of Acronyms and Abbreviations

AGW	Artificial Groundwater
ANS	American Nuclear Society
ANSI	American National Standards Institute, Inc.
APHA	American Public Health Association
ARP	Actinide Removal Process
ASTM	American Society for Testing and Materials
BFS	Blast Furnace Slag
CNWRA	Center for Nuclear Waste Regulatory Analyses
DIW	Deionized Water
DLM	Dynamic Leaching Method
DOE	Department of Energy
EPA	Environmental Protection Agency
ICP-MS	Inductively Coupled Plasma-Mass Spectrometer
LI	Leachability Index
MCU	Modular Caustic Side Solvent Extraction Unit
ORP	Oxidation Reduction Potential
PA	Performance Assessment
psi	per square inch
QA	Quality Assurance
QC	Quality Control
SD	Standard Deviation
SDF	Saltstone Disposal Facility
SDU	Saltstone Disposal Unit
SHC	Saturated Hydraulic Conductivity
SREL	Savannah River Ecology Laboratory
SRR	Savannah River Remediation LLC
SRS	Savannah River Site
UHP	Ultra-High Purity
USEPA	United States Environmental Protection Agency
VZP	Vadose Pore-Water Solution

2.0 Introduction

Reactivity and saturated hydraulic conductivity (SHC) are important factors controlling the rate of weathering and stability of cementitious materials used for the long-term disposal of low-level radioactive wastes. At the Savannah River Site (SRS) chemically reducing materials, such as blast furnace slag (BFS), are added to saltstone grout formulations mixed with low-level radioactive saltwaste materials in order to enhance the attenuation of redox sensitive contaminants, e.g., technetium (^{99}Tc). The persistence of chemically reducing conditions within the grout is an important factor driving long-term risk potential in the Performance Assessment (PA) for the Saltstone Disposal Facility (SDF). The residual reductive capacity of saltstone materials is a function of the grout formulation (i.e., the type and amount of reductive components like BFS), curing conditions, and the degree to which subsequent exposure to gaseous or dissolved O_2 is restricted, an obvious function of the material's SHC.

Several studies have demonstrated both the difficulty in reducing pertechnetate (TcO_4^-; i.e., Tc(VII)), the oxidized form of Tc, and the rapid oxidation of reduced Tc (i.e., Tc(IV)) when exposed to even moderate levels of O_2 (Cantrell and Williams, 2013; Kaplan et al., 2011; Kaplan et al., 2008; Almond et al., 2012; Lukens et al., 2005; Ochs et al., 2016). To illustrate the general complexity of the saltstone system, several important redox potentials are provided in Table 1. By convention, standard redox potential reactions are written as reduction reactions. The more positive a given redox potential, the more likely it will be reduced, i.e., proceed to the right. In aqueous systems O_2 and H_2 constrain the limits in terms of achievable levels of oxidation and reduction, respectively. Dissolved sulfides are generally thought to control the redox environment of pore water in slag rich cements (Atkins and Glasser, 1992; Ochs et al., 2016).

Table 1. Standard redox potential for several important reactions at 25 °C and 1 atm (Stumm and Morgan, 1995).

Reaction	$E°, Volt$
1. $ReO_{4(aq)}^- + 4H^+ + 3e^- \leftrightarrow ReO_{2(s)} + 2H_2O_{(l)}$	-0.55
2. $TcO_{4(aq)}^- + 4H^+ + 3e^- \leftrightarrow TcO_{2(s)} + 2H_2O_{(l)}$	-0.361
3. $Fe^{2+} + 2e^- \leftrightarrow Fe_{(S)}$	-0.44
4. $CrO_4^{2-} + 4H_2O + 3e^- \leftrightarrow Cr(OH)_3 + 5OH^-$	-0.13
5. $2H^+ + 2e^- \leftrightarrow H_2$	0.00
6. $Fe^{3+} + e^- \leftrightarrow Fe^{2+}$	+0.77
7. $Fe(OH)_3 + 3H^+ + e^- \leftrightarrow Fe^{2+} + 3H_2O$	+0.98
8. $O_{2(g)} + 4H^+ + 4e^- \leftrightarrow 2H_2O$	+1.23

Figure 1 provides a solubility diagram of important Tc solids thought to control $Tc_{(aq)}$ levels as a function of pH at a pε of 4. In this instance pε is an indicator of redox intensity that is similar to pH, where pε is the hypothetical electron activity, i.e. pε = -log(e). Many of the previous experiments associated with the ability of saltstone to reduce and immobilize Tc have been conducted using ground

saltstone materials as sorbents, a practice that is likely to expose new surfaces to oxidation and alter sorbent properties in an unpredictable manner. In addition, controlled H_2 atmospheres have been used as a means of restricting O_2 exposure for studies evaluating contaminant partitioning despite the fact H_2 may serve as a general chemical reductant and may alter the redox speciation of the target contaminants (i.e., Tc, Cr, Pu, etc.) and other important chemical elements (i.e., Fe, Mn, etc.) in the presence and even absence of the test sorbent, i.e., soil, saltstone, etc.

Figure 1. Solubility diagram for select Tc phases as a function of pH (25 °C) and a p*ε* of 4.

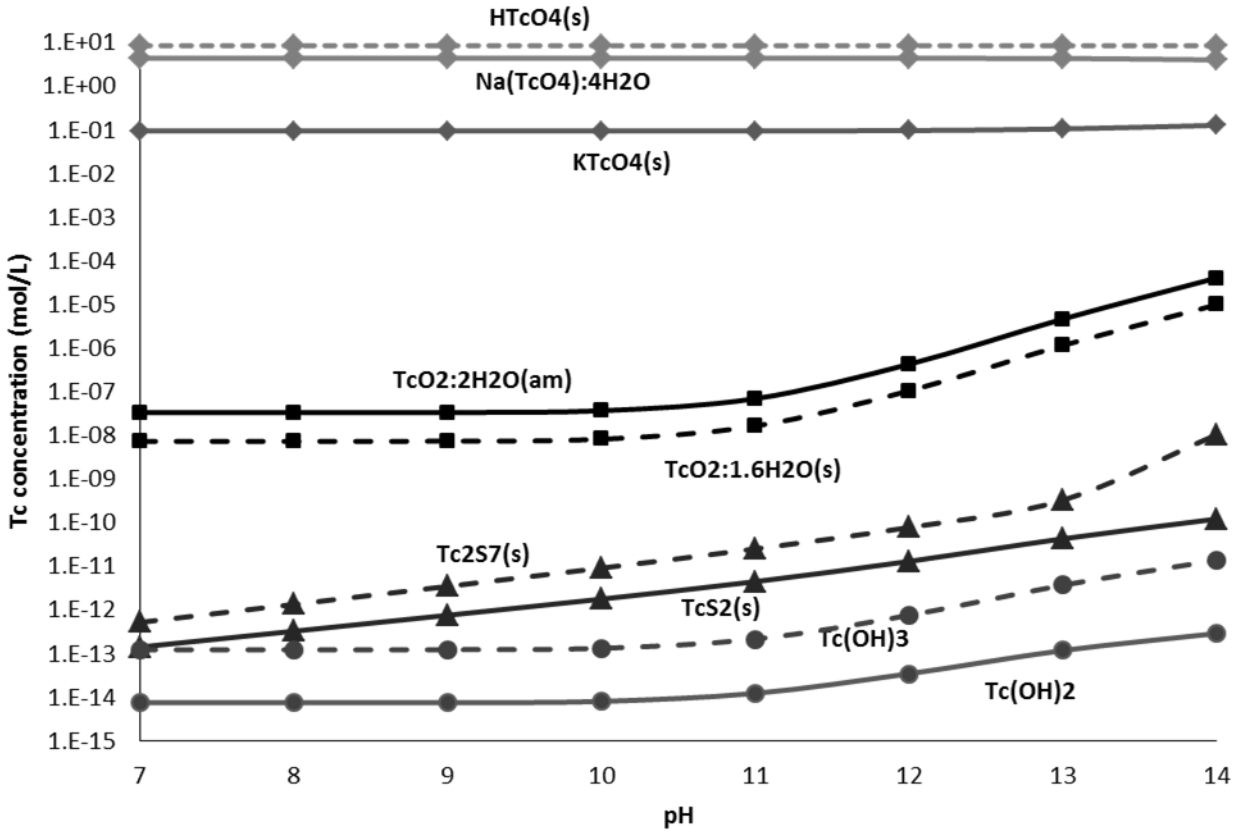

Data generated using PHREEQC-2 and the modified Lawrence Livermore National Laboratory (LLNL) thermodynamic data base (thermo.com.V8.R6.230) prepared by Jim Johnson. The dissolution equation from Cantrell et al. (2013) for TcO_2:1.6H_2O(s) was also included.

To address such issues, the United States Environmental Protection Agency (USEPA; EPA for short) Method 1315, *Mass Transfer Rates of Constituents in Monolithic or Compacted Granular Materials Using a Semi-Dynamic Tank Leaching Procedure* (USEPA 2013), was developed for evaluating the leaching potential of contaminants found in cementitious materials (Garrabrants et al., 2014; Kosson et al., 2014; Serne et al., 2015). EPA Method 1315 is similar to American National Standards Institute, Inc./American Nuclear Society Method 16.1 (ANSI/ANS16.1), *Measurement of the Leachability of Solidified Low-Level Radioactive Wastes by a Short-Term Test Procedure* (ANS 2003), with the leaching intervals modified to accommodate a more complex interpretation of contaminant release mechanisms. Both methods are seen as vast improvements over previous tests

using size-reduced materials that focus on equilibrium partitioning rather than the rate of contaminant release under physically realistic conditions.

The leaching potential of contaminants from solid waste, including "size-reduced" cementitious materials, has previously been evaluated using the batch extraction method defined in EPA Method 1311, *Toxicity Characteristic Leaching Procedure* (TCLP) (USEPA 1992). The TCLP method was designed to represent the leaching conditions present in a municipal waste landfill scenario. However, contaminant mass transport in monolithic materials is controlled by diffusion through the tortuous pore network combined with the aqueous phase partitioning reactions at the solid/solution interface (i.e., adsorption/desorption, precipitation/dissolution, complexation reactions, etc.).

As noted above, the physical structure of the saltstone material combined with maintaining a high degree of saturation serves as a barrier against exposure to O_2. Grinding saltstone for sorption/desorption tests, and even removal from high humidity environments, may facilitate contaminant oxidation and the consumption of saltstone's inherent reductive capacity. The objective of the current study was to evaluate the leaching behavior of ^{99}Tc and other contaminants from spiked saltstone simulant monoliths in comparison with actual intact saltstone samples collected from SDF-SDU Cell 2A.

3.0 Materials and Methods

3.1 SDU Cell 2A Core Extraction

Samples of field-emplaced saltstone from the SDF were collected in April-May 2015 to support ongoing SDF PA activities. As summarized in Simner (2016, SRR-CWDA-2016-00051), a set of emplaced saltstone core samples were collected from SDU Cell 2A (SDU-2A) approximately 20 months after the materials had been poured. The core samples were collected using a wet core drilling method. The goal of the sampling effort was to collect saltstone materials that retained the chemical and physical properties of emplaced saltstone for comparison with laboratory-prepared samples that are often used as surrogates for predicting SDU behavior. The retrieved samples were immediately placed in a moist N_2 environment to prevent oxidation prior to testing. Three of the SDU core samples were included in the current study for comparison, designated SDUA, SDUB and SDUC which corresponds to original sample designations of SDU2A-0931-C-1-U-2, SDU2A-0931-C-1-U-5, and SDU2A-0931-C-2-U-2, respectively. A more thorough description and inventory of the samples from SDU-2A can be found in SRNL-L3100-2015-00108 Rev. 0.

3.2 Contaminant Mass Transfer: EPA Method 1315: Mass Transfer Rates for Monolithic Samples

EPA Method 1315, a semi-dynamic tank leaching procedure, was used to evaluate ^{129}I leaching from SDU Cell 2A saltstone monoliths. EPA Method 1315 is similar to ANSI/ANS16.1 (2003) with modified leaching intervals that potentially allow for a more-complicated interpretation of processes controlling contaminant release over the course of testing. Prior to testing, the SDU samples were sectioned to conform to the EPA 1315 Method recommendations and provide subsections for additional testing, e.g., DLM testing, chemical analysis, etc. The ^{99}Tc and ^{137}Cs results for EPA 1315 tests were presented in a previous report (Seaman et al. 2016). Due to analytical limitations, the EPA Test leachates for the SDU Cell 2A samples were shipped to GEL Laboratories (Charleston, SC 29407) for ^{129}I analysis. The relevant properties of the saltstone materials used for EPA 1315 testing are provided in Table 2.

Table 2. Physical and chemical properties of spiked saltstone simulants and saltstone samples from SDU Cell 2A that were tested using EPA Method 1315.

Sample	Curing Duration	BFS Materials	Mass (gm)	1315 Exposed Surface Area (cm^2)	^{99}Tc** ($pCi\ gm^{-1}$)	^{129}I*** ($pCi\ gm^{-1}$)	^{137}Cs**** ($pCi\ gm^{-1}$)
FY16 Data ^{99}Tc Spiked Saltstone							
Tc2	3 Months	Lehigh	267	164	6.7E+03	NA	NA
Tc6	6 Months	Lehigh	261	156	6.7E+03	NA	NA
Tc4 (1D)	6 Months	Lehigh	175	20	6.7E+03	NA	NA
Tc9	3 Months	Holcim	288	168	6.7E+03	NA	NA
SDU Cell 2A Samples							
SDU-A	≈20 Months#	Holcim	272	168	6.4E+03	4.13	7.9E+05
SDU-B	≈20 Months#	Holcim	272	168	6.4E+03	4.13	4.8E+05
SDU-C	≈20 Months#	Holcim	360	208	6.4E+03	4.13	4.9E+05

*Average of test replicates performed under three different atmospheres

**Tc-99 levels in SDU saltstone based on spike levels for laboratory samples and Tank 50 composition for SDU samples (i.e., Bannochie, 2014)

***I-129 levels based on the average concentration reported by SRNL for analysis of nine SDU2A core samples (SRNL-L3100-2015-00108 Rev. 0.)

***Cs-137 levels based on analysis of sectioned SDU samples

#approximately 20 months curing in SDU Cell 2A plus additional curing after sample collection before testing began

Sample SDU-A = SDU2A-0931-C-1-U-2

Sample SDU-B = SDU2A-0931-C-1-U-5

Sample SDU-C = SDU2A-0931-C-2-U-2

The terminology adopted by Serne et al. (2015) was used to refer to the EPA leaching tests, with leachant referring to the starting solution used to interact with the saltstone, and leachate to refer to the resulting solution after contact with saltstone. An artificial groundwater (AGW; see Table 3) surrogate based on routine sampling of non-impacted water table wells on the SRS (Strom and Kaback, 1992) was used as the leachant for the EPA 1315 test and the leaching solution for the DLM experiments described in the subsequent text. In preparation for additional saltstone leaching tests in the future, a test solution is being developed to mimic the composition of soil water that has been in

contact with SDU concrete. An SDU concrete test monolith was crushed and sieved to provide a range of concrete particle sizes, i.e., a large intact concrete aggregate, > 2 mm, 1-2 mm, and < 1 mm. Approximately 15 gm of each sized material was added to separate flasks containing 150 mL of AGW and the shaken on an orbital shaker for a week. The water samples were then filtered and analyzed for major elements by ICP-MS (NexION 300, Perkin Elmer, Inc.). The final concentration for the equilibrated SDU Concrete/AGW solutions is provided in Table 4. This data will potentially be used to evaluate future SDU leaching scenarios.

The mass transfer tests were conducted at room temperature (i.e., 22 ± 2 °C) under ambient laboratory atmosphere. Previous studies detailed in Seaman (2015) demonstrated that ^{99}Tc leaching from monolithic saltstone simulants was generally insensitive to the test atmosphere. The volume of eluent used in each leaching interval conformed to the liquid-to-surface area ratio (L/A) of 9 ± 1 mL cm^{-2} dictated by EPA Method 1315, and the test leachant was replaced with fresh solution according to the schedule provided in Table 5.

Table 3. Composition of the artificial groundwater (AGW) simulant.

Constituent/Parameter	AGW[a]
pH	5.0
	(mg L^{-1})
Na	1.39
K	0.21
Ca	1.00
Mg	0.66
Cl	5.51
SO_4	0.73

[a]Artificial Groundwater: non-impacted groundwater derived from natural infiltration (Strom and Kaback, 1992)

Table 4. Composition of various size fractioned SDU Construction concrete equilibrated with artificial groundwater (AGW) simulant.

Constituent/Parameter	Single Aggregate	>2 mm	1 to 2 mm	< 2 mm
pH	11.3	11.3	11.3	11.4
	(mg L^{-1})			
Na	6.44	10.8	13.2	14.7
K	13.8	21.9	26.3	27.9
Ca	47.1	63.7	76.1	90.6
Mg	0.19	0.15	0.09	0.10

Table 5. Schedule for fresh leachate renewals for EPA 1315.

Interval Label	Interval Duration (h)	Interval Duration (d)	Cumulative Leaching Time (d)
T01	2.0 ± 0.25		0.08
T02	23.0 ± 0.5		1
T03	23.0 ± 0.5		2
T04		5.0 ± 0.1	7
T05		7.0 ± 0.1	14
T06		14.0 ± 0.1	28
T07		14.0 ± 0.1	42
T08		7.0 ± 0.1	49
T09		14.0 ± 0.1	63

The choice of an appropriate leachant solution can have a significant impact of test results. In similar studies Serne et al. (2015) found that contaminant leaching in the presence of a vadose zone pore-water simulant (VZP) derived for Hanford was lower when compared to DIW, which they attributed to precipitates observed forming at the Cast Stone surface. The precipitate was later identified predominantly as aragonite (a polymorph of calcium carbonate), with some brucite ($Mg(OH)_2$), and possibly calcite ($CaCO_3$) that hindered contaminant diffusion. No such precipitate was observed using an SRS groundwater surrogate in the current study (i.e., AGW), which has a much lower overall ionic strength as well as lower Ca and Mg levels than the Hanford VZP.

3.4 Leachate Data Analysis

The effective diffusivity, D_e (cm/s^2), for ^{129}I and the other saltwaste contaminants (i.e., ^{137}Cs and NO_3^-) was calculated using the simplified approach outlined in ANSI/ANS-16.1 (ANSI/ANS, 2003):

$$D_e = \pi \left[\frac{a_n / A_0}{\Delta t_n} \right] \left[\frac{V}{S} \right]^2 T \qquad [1]$$

where a_n is the quantity of contaminant released during interval n, A_0 is the total quantity of contaminant initially present in the sample being tested, Δt_n is the duration of the n^{th} interval, V is the volume of the sample (cm^3), S is the surface area of the sample (cm^2), and T is the generalized mean square root of the leaching time:

$$T = \left[\frac{\sqrt{t_n} + \sqrt{t_{n-1}}}{2} \right]^2 \qquad [2]$$

where t_n is the elapsed time at the end of the current sampling interval and t_{n-1} is the elapsed time at the end of the previous sampling interval. The approach outlined above using the incremental fraction of

the contaminant leached during each interval provides an estimate of diffusivity for each sampling interval that is independent of the other sampling intervals, and not subject to any bias that may occur during early sampling times when surficial materials may be released. Additionally, a more-specific solution that accounts for the geometry of the specimen is required when more > 20% of the contaminant has leached from the sample (ANSI/ANS, 2003). When greater than 20% of the initial contaminant inventory has been leached from the sample, as is often seen for NO_3^-, the release data become non-linear with the square root of time due to depletion, and are not included in estimates of diffusivity.

For comparison, the leachability index (LI), a unit-less parameter derived from the effective diffusion coefficient, i.e., D_e (cm^2/s), was calculated using the equation presented in Serne et al. (2015):

$$LI_n = -\log[D_e] \quad [3]$$

where LI_n is the leachability index for sampling interval n. The reported LI values in the current study reflect the average for all sampling intervals where less than 20% of the initial contaminant of interest has been leached from the intact sample. It is important to note that the "diffusional" release of retained contaminants from cementitious waste reflects a combination of both chemical and physical transport processes, such as dissolution or desorption, in response to changes in pore solution composition combined with diffusional transport. A LI value of 6 or greater is generally considered the threshold for a given matrix as adequate for immobilization of radioactive wastes (Serne et al., 2015).

3.3 ^{99}Tc Spiked Saltstone Formulations for DLM Testing

Technetium-99 spiked saltstone used in the DLM experiments was produced using a saltwaste simulant recipe specified by SRR (Table 6) and then subjected to a temperature/humidity curing profile that mimicked the environmental conditions in a SDU Cell 2B (Figure 2). The relative concentrations of ^{99}Tc in the saltwaste simulant (≈ 2 x 10^4 pCi mL^{-1}) were consistent with the average concentrations of ^{99}Tc in the Tank 50 feed waste at the SDF (Bannochie, 2012, 2014). The dry feed materials consisted of (1) Class F fly ash (The SEFA Group, Inc. Lexington, SC 29073), (2) Grade 100/120 blast furnace slag (Holcim US, Inc. Birmingham, AL 35221), and (3) Type II Portland cement (Holcim US, Inc. Birmingham, AL 35221). The dry feed material ratio was 45% fly ash, 45% BFS and 10% Portland cement

All of the chemicals in Table 6, except for the NaOH solution, were combined with ≈ 0.5 L of deionized water (DIW) in multiple 1-L volumetric polycarbonate flasks depending on the total mass of saltstone being created. The NaOH was then added as a 50% solution. The contaminant spike solution was added to the saltwaste flasks just before making up the solution to its final volume. Spike concentrations are consistent with the average levels of ^{99}Tc found in Tank 50 saltwaste (Bannochie, 2012, 2014). The following day, the required masses of the three powdered grout materials were weighed in three separate containers. The three dry powdered materials were then mixed together in a

single bucket. After thorough homogenization of the combined dry powders, the saltwaste simulant solution was slowly added to the dry materials while mixing at 250 rpm for 20 minutes.

The saltwaste solution was added at a water to dry materials ratio of 0.6. After mixing, the ^{99}Tc spiked slurries were poured into several 2" ID x 4" L plastic concrete molds and sealed with plastic lids for curing (Test Mark Industries, Inc.). The plastic concrete molds were then placed in a humidity-controlled curing oven (Model 6105, Caron Products & Services, Inc.) and heated according to the curing profile from SDU Cell 2B (Figure 2) (Simner, 2016).

Table 6. Composition of ARP/MCU saltwaste simulant.

Material	Molarity (moles/L)	Mass for 1L (g/L)
Sodium Hydroxide, 50 wt% NaOH	**1.594**	**127.52**
Sodium Nitrate, $NaNO_3$	**3.159**	**268.52**
Sodium Nitrite, $NaNO_2$	**0.368**	**25.39**
Sodium Carbonate, Na_2CO_3	**0.176**	**18.66**
Sodium Sulfate, Na_2SO_4	**0.059**	**8.38**
Aluminum Nitrate, $Al(NO_3)_3.9H_2O$	**0.054**	**20.25**
Sodium Phosphate, $Na_3PO_4.12H_2O$	**0.012**	**4.56**

Figure 2. Curing profile for Saltstone Disposal Unit (SDU) Cell 2B (Simner, 2016).

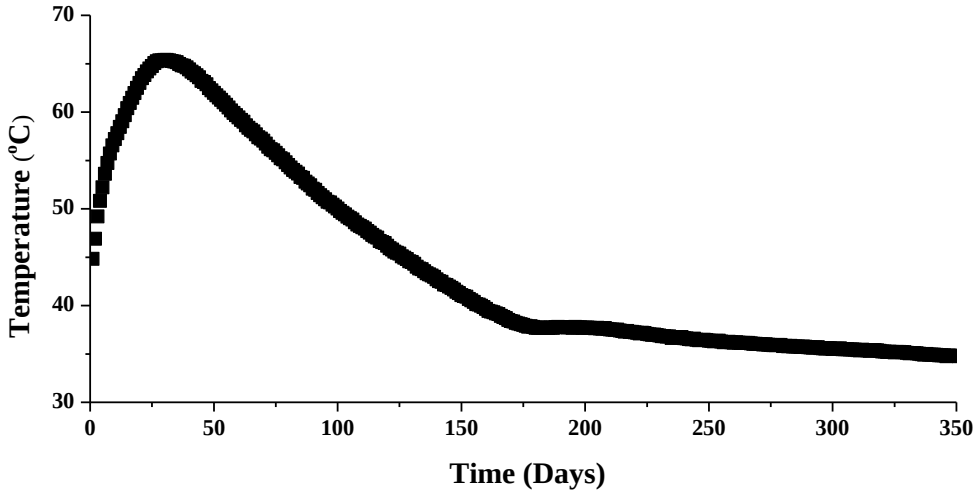

3.5 Dynamic Leaching Method

The Dynamic Leaching Method (DLM) is based on ASTM D5084 for determining the SHC of cementitious materials using a flexible-wall permeameter to develop the necessary hydraulic gradient and ensure internal flow (Figure 3). Darcy's Law was used to establish the initial leaching conditions:

$$q = \frac{Q}{A} = \frac{K\Delta H}{L} \quad [4]$$

where q is the flux density (i.e., volume flowing through a specific cross-sectional area), Q ($cm^3\ sec^{-1}$) is the discharge volume per unit time (i.e., V/t), A is the cross sectional area (cm^2), K ($cm\ sec^{-1}$) is the hydraulic conductivity, ΔH is the hydraulic head difference between the column inlet and outlet (i.e., $\Delta H = H_i - H_o$; cm), and L is the length of the column (cm) (Hillel, 1980).

Given a two-inch diameter saltstone monolith (i.e., cross-sectional area of 20.27 cm^2) with a core length of one inch (2.54 cm), and an assumed SHC of 5 x 10^{-9} cm sec^{-1}, the pressure required to achieve a leaching rate of approximately 5 mL per day (i.e., 5.79 x 10^{-5} $cm^3\ sec^{-1}$) can be calculated as:

$$q = \frac{Q}{A} = \frac{5.79\times10^{-5} cm^3 s^{-1}}{20.27\ cm^2} = 2.86 \times 10^{-6} cm\ s^{-1} = \frac{K\Delta H}{L} \quad [5]$$

The equation is then solved for ΔH, the required hydraulic gradient in cm.

$$\Delta H = \frac{qL}{K} = \frac{2.86\times10^{-6} cm\ s^{-1} L}{K} = \frac{2.86\times10^{-6} cm\ s^{-1}\times 2.54\ cm}{5\times10^{-9} cm\ s^{-1}} = 1453 cm \quad [6]$$

The hydraulic gradient is then converted to psi.

$$psi = \frac{1453 cm}{70.38\ cm\ psi^{-1}} = 20.61\ psi \quad [7]$$

Changes in the relative SHC during the course of leaching can be estimated using Darcy's equation based on the set hydrostatic pressure at the column inlet and the observed effluent flow rate. The porosity of each sample was determined by the mass loss of water upon heating samples to 105 °C in a laboratory oven, with samples measured repeatedly until the mass change on consecutive days was <5% (Westsik et al., 2013). For the current saltstone materials, the average % moisture content ≈ 58%, consistent with other estimates for similar materials (Westsik et al., 2013). This was used as an estimate of sample pore volume (PV) for comparing sample monoliths of differing dimensions.

Technetium-99 (^{99}Tc) present in the DLM leachates was analyzed by liquid scintillation counting (LSC) according to ASTM D7283-13, *Standard Test Method for Alpha and Beta Activity in Water by Liquid Scintillation*, using a Beckman/Coulter LS6500 (ASTM, 2013). Cesium-137 present in the leachates from the SDU Cell 2A samples was determined by gamma spectrometry. Nitrate leaching for the SDU and ^{99}Tc-spiked gout samples was monitored using the chromotropic acid test

method, *APHA Method-4500-Nitrogen, Standard Methods for the Examination of Water and Wastewater* (APHA, 1997).

Figure 3. Diagram of the original DLM testing apparatus (A) showing the flex-wall permeameter cell, inlet leachate source, and sample collection outlet. Revised DLM apparatus (B) with mechanical pumps (Geocomp, Inc.) to provide constant stable flow as back-pressures vary.

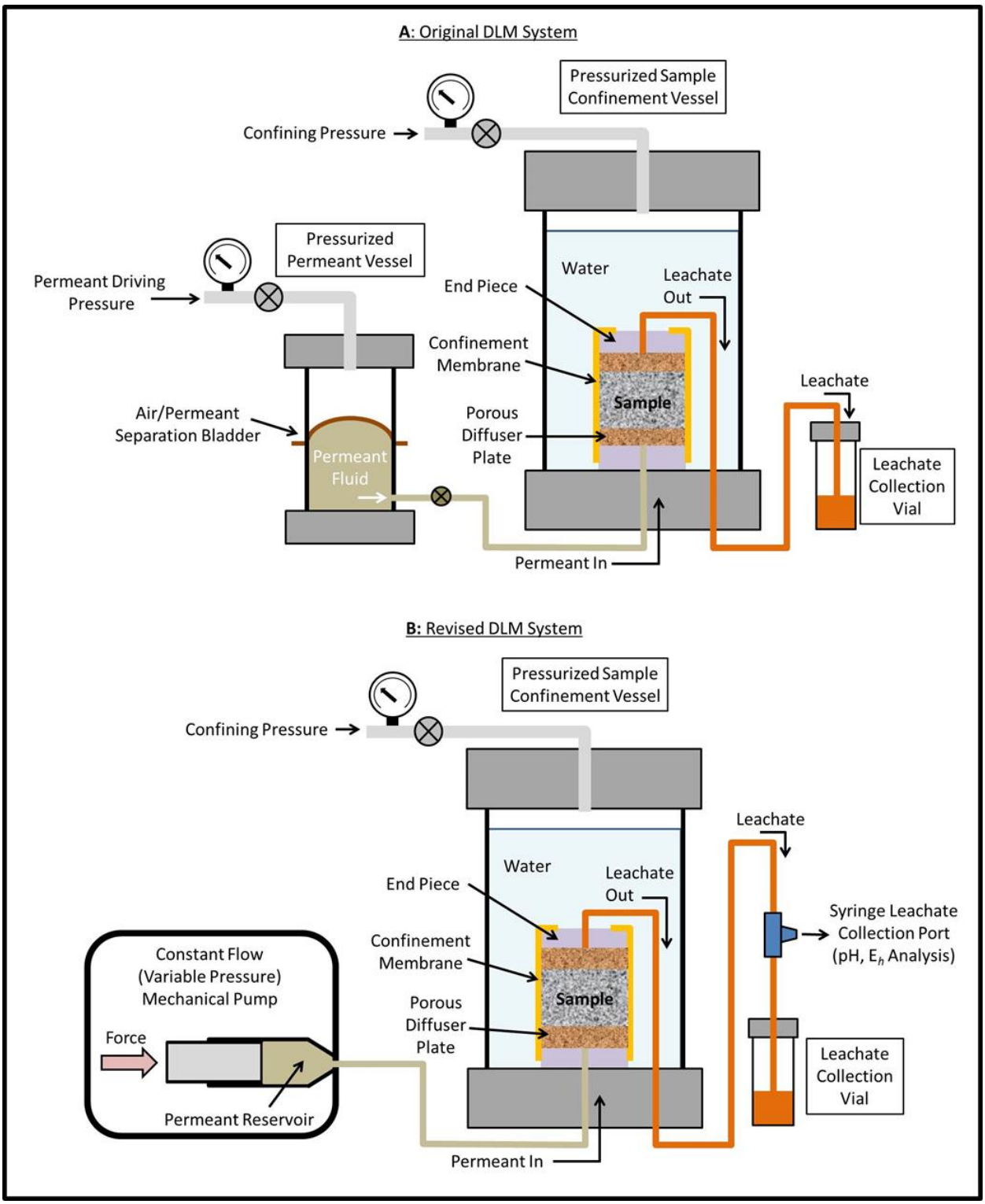

4.0 Results

4.1 EPA Method 1315

An updated summary of the data for all EPA leaching tests is provided in Appendix A. Plots of the logarithm of cumulative release rate for ^{129}I as function of the logarithm of leaching time generally yield negative slopes of 0.5 ± 0.15, indicative of a "diffusion" controlled process (USEPA, 2013). Adherence to the linear release model simplifies comparison of different data sets, without necessarily providing mechanistic information concerning the chemical mechanisms of constituent immobilization and release. However, when greater than 20% of the initial inventory of a specific contaminant has been leached from the sample, the release data generally no longer conform to the diffusional model, and are not included in estimates of diffusivity or the leachability index, *LI*. Such was the case for the last three data points for SDU-A.

4.2 Iodine-129

The measured concentrations of ^{129}I in the EPA 1315 leachate from the three SDU Cell 2A samples are presented in Figure 4A, with the cumulative leaching fraction in 4B. The ^{129}I leaching patterns were similar to those observed for both ^{137}Cs and NO_3^-, with two of the three samples yielding similar leachate concentrations (SDU-B and SDU-C), while the third was noticeably higher (SDU-A). The higher degree of ^{137}Cs leaching for SDU-A was attributed to the greater initial ^{137}Cs concentration in the saltstone (7.9×10^5 pCi gm^{-1}), with both SDU-B and SDU-C having about 4.8×10^5 pCi gm^{-1} (See Table 2). The average reported ^{129}I concentration in Tank 50 at the time these materials were poured, the third quarter of 2013, was 14.3 pCi mL^{-1} (Bannochie, 2014). The concentration in the resulting saltstone can be generally estimated by dividing the tank waste concentration by three, i.e., ≈ 4.77 pCi gm^{-1}. However, the ^{129}I concentration in the SDU-2A samples was assumed to be the average of nine SDU-2A samples analyzed by SRNL, 4.13 pCi gm^{-1} (SRNL-L3100-2015-00108 Rev. 0.).

The ^{129}I effective diffusivity values, D_e, ranged from 2.5×10^{-9} to 1.0×10^{-8} cm^2 sec^{-1} with *LI* values of 8.0, 8.6, and 8.4 for SDU-A, SDU-B, and SDU-C, respectively (see Table 7). These values are quite similar to those observed for NO_3^- in the current study. Cumulative ^{129}I leaching was high enough for sample SDU-A that the last few data points were excluded in the estimates of D_e and *LI*. Westsik et al. (2013) reported effective diffusivities for Cast Stone monoliths that were in the range of 1×10^{-8} to 2×10^{-9} cm^2 s^{-1}, corresponding to LI values of 8.0 to 8.7, essentially the same as observed in the current study. Westsik et al. (2013) also reported the same range of effective diffusivities for sodium (Na^+), NO_3^- and nitrite (NO_2^-), saltwaste constituents assumed to be poorly sorbed in cementitious grouts. Mattigod et al. (2011) also reported very limited retention of iodine in Cast Stone, with initial diffusivities that ranged from 1×10^{-7} cm^2 s^{-1} to ~3×10^{-7} cm^2 s^{-1} after 90 days of curing.

Figure 4. Leaching results for ^{129}I from EPA Method 1315 for three SDU Cell 2A monoliths: (A) eluate concentration, (B) cumulative ^{129}I leaching from the monoliths.

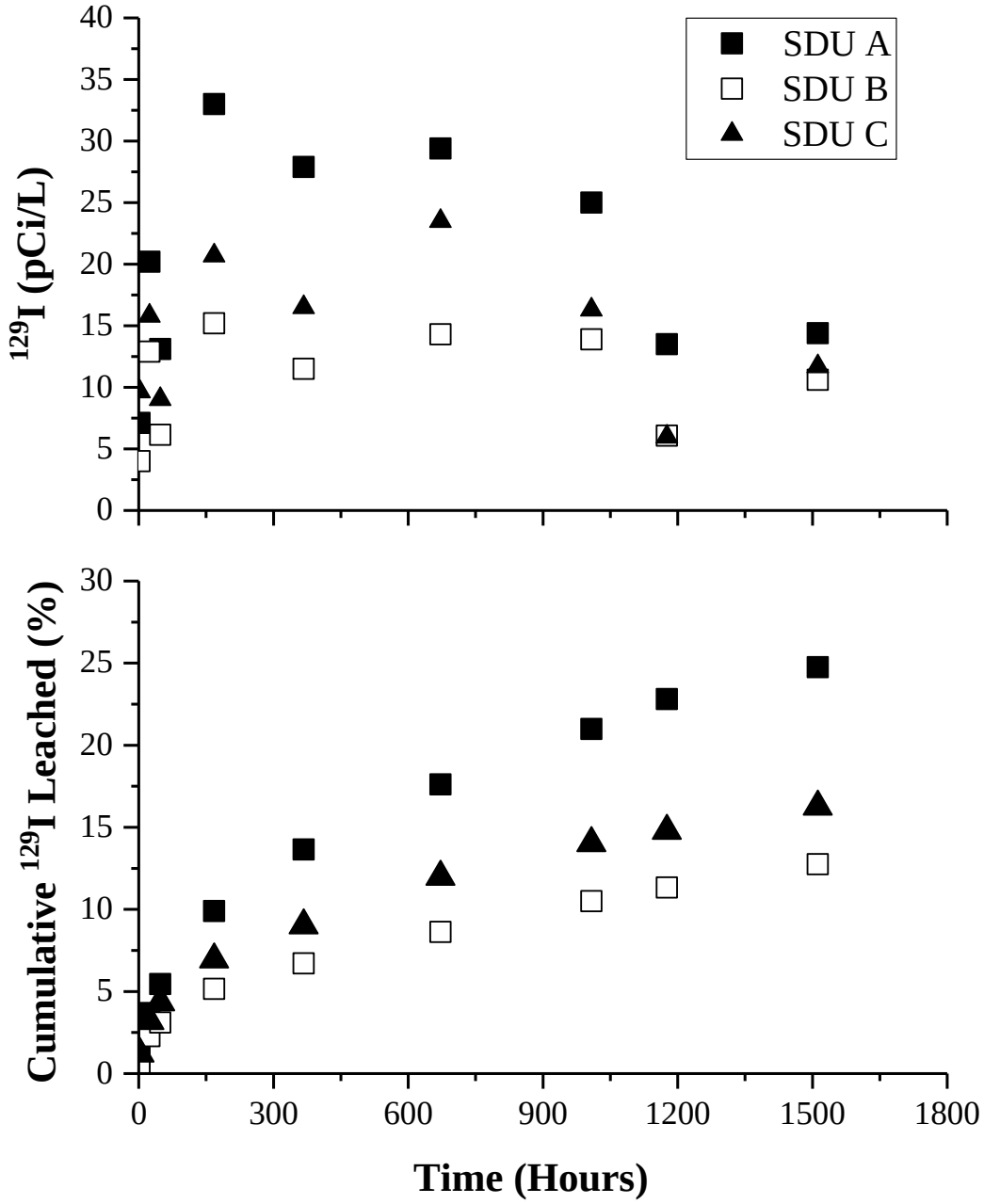

Table 7. Summary of effective diffusivities (D_e) and leachability indices (LI) derived from EPA 1315.

			^{99}Tc		Re		^{137}Cs		NO_3		^{127}I (Stable Iodine)	
Sample	Curing Duration	Materials	D_e (cm^2/sec)	LI	D_e (cm^2/sec)	LI	D_e (cm^2/sec)	LI	D_e (cm^2/sec)	LI	D_e (cm^2/sec)	LI
FY15 Data*												
	3 Months	Old BFS (Holcim)	2.4E-10	9.9	3.0E-08	7.6	NA	NA	4.4E-08	7.6	2.9E-08	7.7
	6 Months	Old BFS (Holcim)	2.8E-10	9.7	3.3E-08	7.6	NA	NA	1.6E-08	7.9	3.0E-08	7.7
			^{99}Tc		Re		^{137}Cs		NO_3		^{129}I	
FY16 Data**												
Tc2	3 Months	New BFS (Lehigh)	2.6E-11	10.6	NA	NA	NA	NA	4.8E-08	7.5	NA	NA
Tc6	6 Months	New BFS (Lehigh)	5.7E-12	11.3	NA	NA	NA	NA	6.6E-08	7.2	NA	NA
Tc4 (1D)	6 Months	New BFS (Lehigh)	3.8E-11	10.5	NA	NA	NA	NA	2.1E-07	6.7	NA	NA
Tc9	3 Months	Old BFS (Holcim)	3.0E-10	9.6	NA	NA	NA	NA	3.7E-07	6.7	NA	NA
SDU2A Sample A	20 Months**	Old BFS (Holcim)	6.4E-11	10.2	NA	NA	4.2E-10	9.4	1.3E-08	8.0	1.0E-08	8.0
SDU2A Sample B	20 Months**	Old BFS (Holcim)	5.8E-11	10.3	NA	NA	1.1E-10	10.0	4.4E-09	8.5	2.5E-09	8.6
SDU2A Sample C	20 Months**	Old BFS (Holcim)	5.2E-11	10.3	NA	NA	4.9E-10	9.5	5.5E-09	8.5	5.5E-09	8.4

*Reported in Seaman (2015). Reflects the average of test replicates (1D configuration) performed under three diferent atmospheres

NA Not Applicable

Sample A = SDU2A-0931-C-1-U-2

Sample B = SDU2A-0931-C-1-U-5

Sample C = SDU2A-0931-C-2-U-2

4.3 Dynamic Leaching Method

In earlier studies, Seaman and Chang (2014) and Seaman et al. (2015; 2016) developed and refined the DLM method to evaluate contaminant partitioning within intact cementitious materials through the use of a flexible-walled permeameter system to achieve steady saturated leaching through materials with relatively low saturated hydraulic conductivities, i.e., $K_{sat} \leq 1 \times 10^{-9}$ cm sec^{-1}. Recently, the Center for Nuclear Waste Regulatory Analyses (CNWRA) started evaluating similar method for achieving saturated flow in intact saltstone monoliths (Dinwiddie and Pickett, 2017). Seaman et al. (2015; 2016) first utilized the method to demonstrate that Re is a poor analogue for ^{99}Tc, with much greater Re leaching observed from intact samples. Eventually the DLM system was expanded to accommodate the simultaneous testing of three intact samples by using a custom pressure manifold with two control valves dedicated to each sample to control both the confining and leaching pressures (Figure 5). A bladder accumulator was added to the modified system for each test cell to provide a reservoir for the inlet leaching solutions with a flexible membrane that can be used to apply the required driving pressure and restrict leachate exposure to the atmosphere before entering the DLM system (see Figure 3A).

Figure 5. Expandable DLM control manifold with two permeameter cells and associated bladder accumulators installed.

The modified three-sample DLM manifold has been used to continuously leach AGW through a ^{99}Tc-spiked monolith and two ≈ 2.5 cm long x ≈ 5 cm diameter SDU core sections representing samples SDU-A (SDU2A-0931-C-1-U-2) and SDU-B (SDU2A-0931-C-2-U-2). Although there was some initial differences in the ^{137}Cs leaching pattern for the two samples, the relative percentage of cumulative effluent recovery is quite similar (Figure 6), with effluent ^{137}Cs leveling off at about 10% of the total mass in each SDU sample.

Figure 6. Effluent ^{137}Cs and cumulative ^{137}Cs recovery for the two SDU samples.

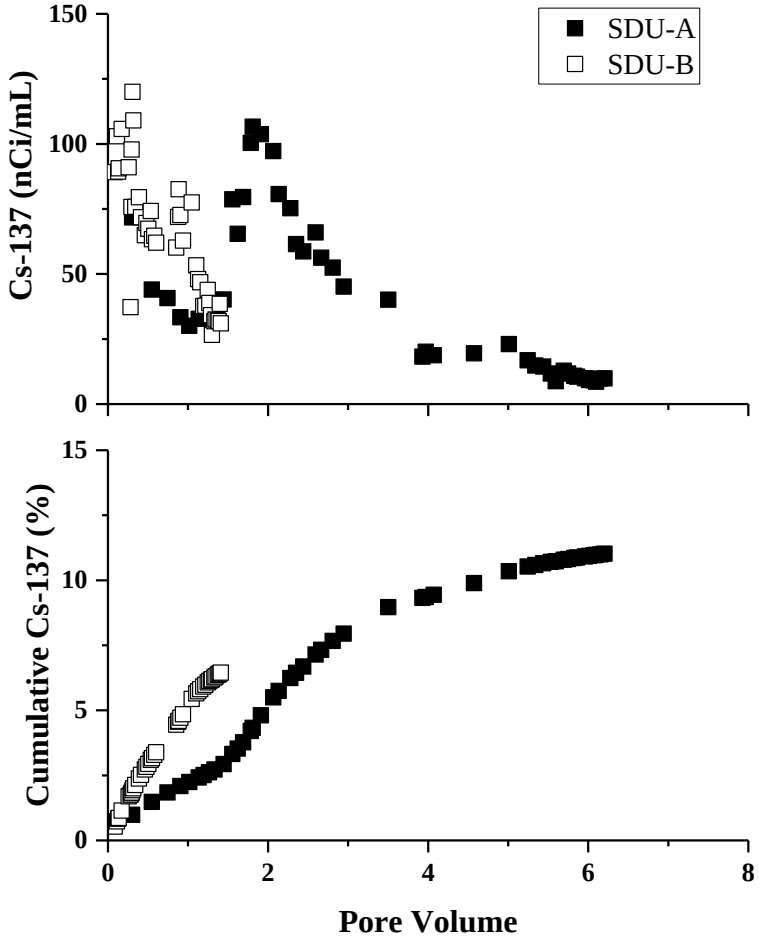

Effluent NO_3^- concentrations and the percentage of NO_3^- recovered in the effluent to date for SDU-A and the ^{99}Tc-spiked sample can be seen in Figure 7. As noted for ^{137}Cs, there appears to be some similarity with respect to the cumulative amount of NO_3^- that can be leached from the sample. It is important to note, however, that the total fraction of ^{137}Cs that has been leached from the two SDU samples is much less than the NO_3^- levels, indicating some form of ^{137}Cs immobilization within the saltstone, consistent with the EPA 1315 leaching test results (Table 5). The *LI* values for ^{137}Cs ranged

from 9.4 to 10 for the SDU samples while the *LI* values for NO_3^- in the SDU samples ranged 8.0 to 8.5, indicating significant ^{137}Cs retention of within saltstone.

Figure 7. Effluent NO_3^- and cumulative percent NO_3^- recovery for one SDU sample (SDU-A) and the ^{99}Tc-spiked sample.

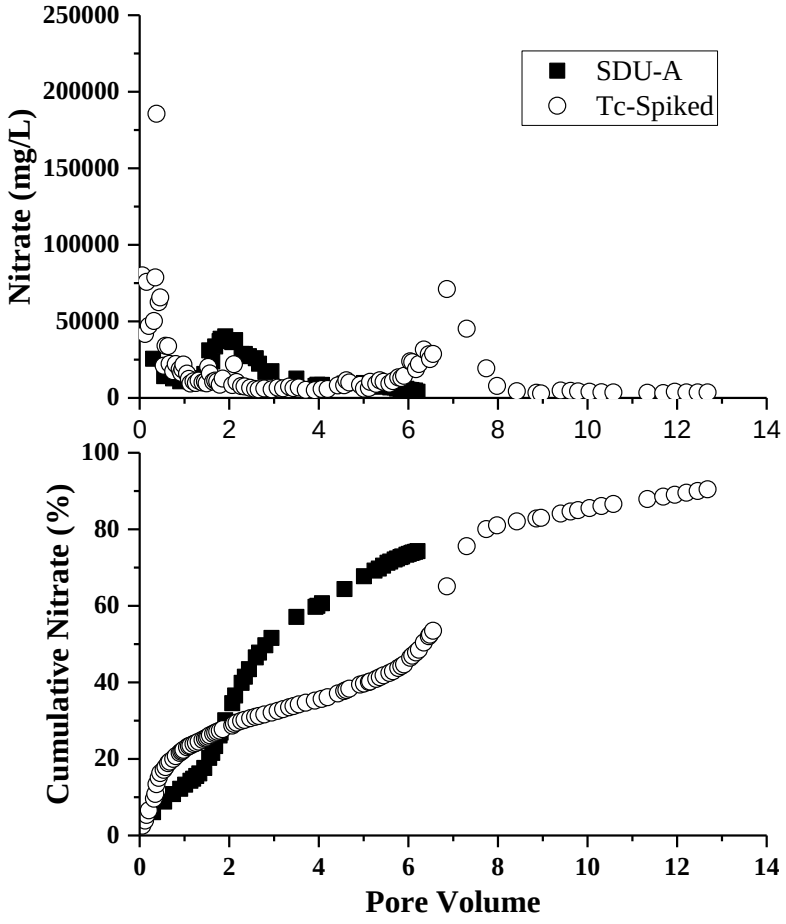

Figure 8 displays the effluent ^{99}Tc concentration and the cumulative effluent ^{99}Tc recovery for the three DLM test materials. The obvious differences in the number of pore volumes leached for the three test samples is indicative of their differences in SHC. Although the leaching pattern for the three materials are somewhat different, it is important to note that the cumulative % of ^{99}Tc recovered is much less than that of NO_3^-, which again is consistent with the EPA 1315 test results. Using a similar leaching system at much higher pressures, Dinwiddie and Pickett reported similar effluent ^{99}Tc levels from an intact, spiked saltstone sample (Dinwiddie and Pickett, 2017).

Figure 8. Effluent ^{99}Tc and cumulative percent ^{99}Tc recovery for the two SDU samples and the ^{99}Tc-spiked sample.

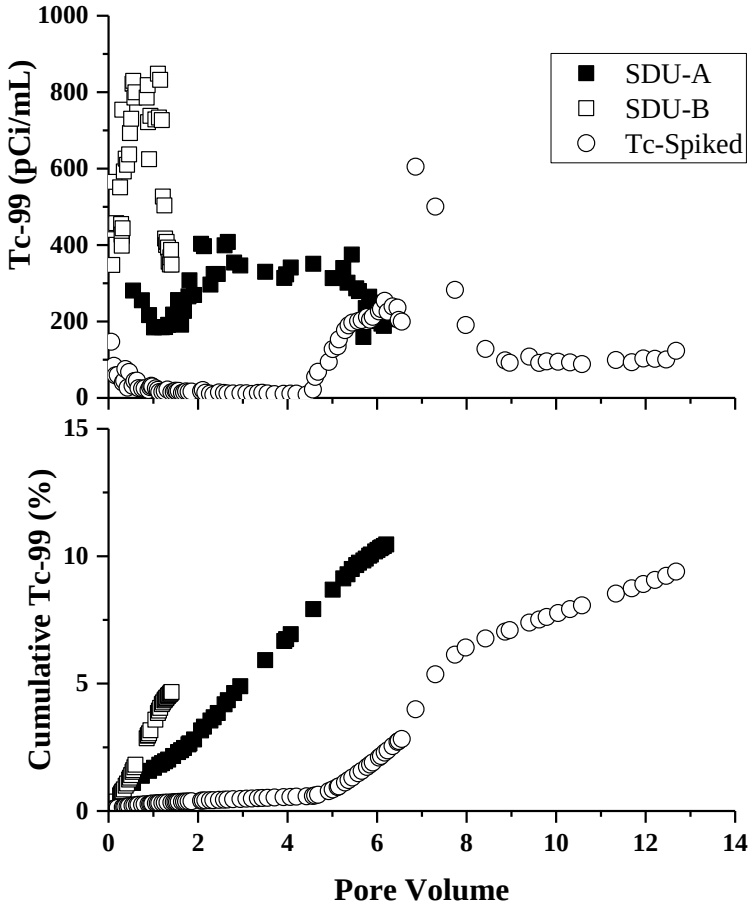

As noted above, it is quite difficult to maintain a constant flow rate using the inlet pressure, complicating the interpretation of results because of different leachate residence times depending on the materials K_{sat}. Figure 9 provides the percent recovery for the three effluent constituents that were monitored for SDU sample SDU-A. It is interesting to note that all three constituent display similar effluent leaching patterns despite the large differences in their total recovery and presumably different mechanisms of sorption within the saltstone. This suggests that some of the transitional shifts in the recovery of the three constituents are controlled by physical changes within the system that impact all three in a similar manner.

Figure 9. Percentage of NO_3^-, ^{137}Cs and ^{99}Tc recovered in the effluent of SDU sample SDU-A.

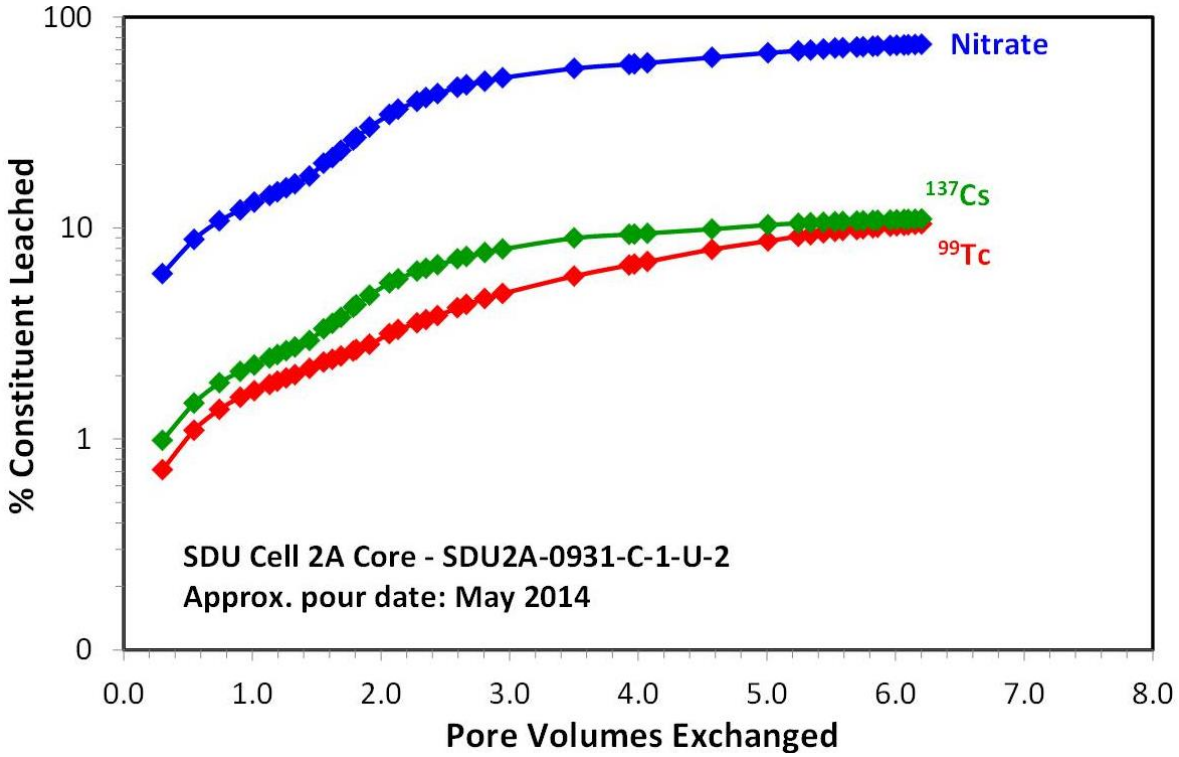

Reliably monitoring the pH and ORP for effluents from the DLM columns is critical in evaluating the leaching behavior for saltwaste constituents that are redox and pH sensitive, like ^{99}Tc. However, initial pH and ORP readings for effluent samples were inconsistent with elevated ^{99}Tc levels in a reducing system and even initial weathering patterns of fresh cementitious materials. For example, some of the initial pH values were ≤ 11 , considerably lower than the pH observed for the first two stages of weathering ($pH \geq 12.5$) for hydrated cements (Ochs et al., 2015). In addition, the ^{99}Tc levels were too high for reduced Tc(IV) species like $TcO_2.2H_2O_{(am)}$ or $TcO_2.1.6H_2O_{(s)}$ to be controlling ^{99}Tc solubility. The lower pH is presumably the result of CO_2 adsorbed by the alkaline effluent solutions during the extended sampling times, with anomalously higher ORP values, indicative of a more oxidizing system, resulting from the samples atmospheric exposure to O_2.

In Figure 10 the effluent ^{99}Tc concentration for DLM samples is plotted as a function of the sample pH as determined using the new method over an estimated solubility diagram for various Tc-containing solid phases. The figure illustrates that when atmospheric exposure was limited during sample collection by withdrawing effluent from the tubing prior to collection in the sample vial, the pH was generally one or more units higher and soluble ^{99}Tc levels were consistent with the solubility of $TcO_2.2H_2O(am)$.

Figure 10. Solubility diagram redrawn from Figure 1 highlighting the reduced ^{99}Tc solid phases (i.e., $TcO_2.2H_2O$ or $TcO_2.1.6H_2O$) as a function of pH. Effluent data points (✕) graphed as a function of the pH measured using the new method that restricts atmospheric exposure of the sample.

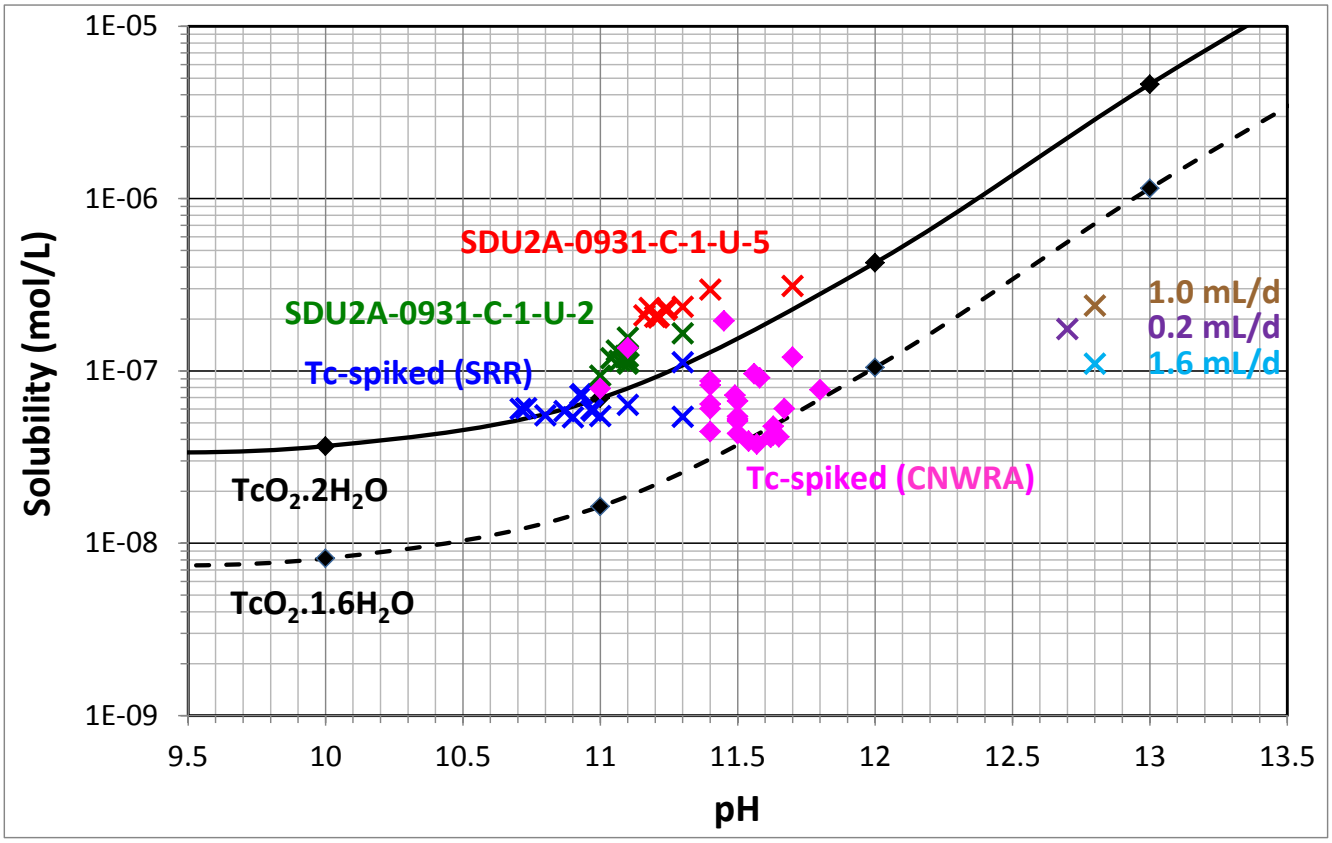

The DLM system was further modified based on the results from extended leaching of the Tc-spiked monolith and two SDU-2A samples (Figure 3B). Instead of using elevated air pressures to both confine the intact sample and drive flow, the system was modified to include a programmable micro-flow pump to maintain constant flow while backpressure in the system can vary due to changes in the SHC of the test sample. A picture of the new test system is provided in Figure 11, with the programmable micro-flow pumps to the left. As with earlier version, compressed air is still used to control the confining pressure holding the flexible membrane in place to restrict by-pass flow. Each pump can be programed to provide a constant flow up to a defined back pressure (i.e., 2 to 3 psi less than the confining pressure) for a defined volume or test duration. At the same time, the pumps constantly monitor and record the inlet pressure, which can be used to calculate the saturated hydraulic conductivity of the sample.

Figure 11. Modified DLM control manifold utilizing three programmable micro-pumps (left) to maintain a constant flow rate for three test samples regardless of the back pressure.

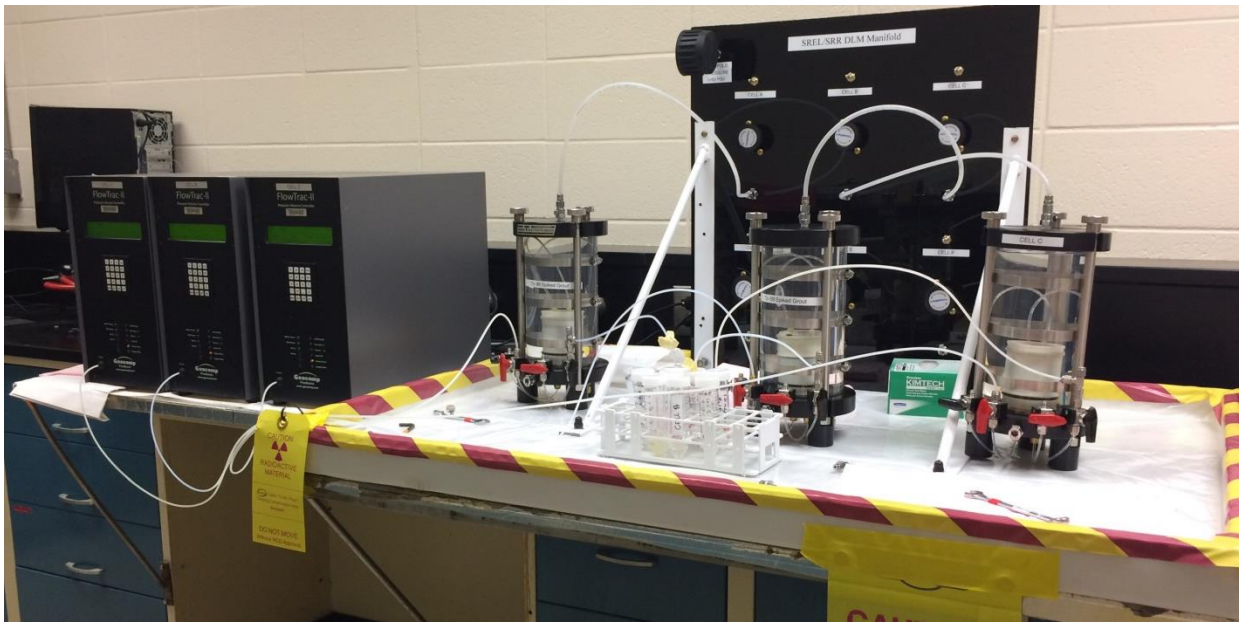

A test of the new DLM system was recently initiated. A set of three ^{99}Tc-spiked saltstone sections from the same curing monolith were mounted in flex-walled permeameters and saturated with AGW according to the protocols of ASTM D5084. After saturation, constant flow (with inlet varying pressure) was initiated at three set flow rates (i.e., 0.2 1.0, 1.6 mL d^{-1}) as part of a controlled test to see the impact of solute residence time on the effluent concentration of ^{99}Tc, as well as effluent pH and ORP, with samples being collected using the modified protocol that limits atmospheric exposure. This residence time experiment conducted at a constant flow should help explain the transient shifts in the concentration of contaminants that was observed in the data set presented above, including the tendency of the effluent concentrations for the monitored constituents (i.e., ^{99}Tc, ^{137}Cs and NO_3^-) to track each other (see Figure 9), although at different relative concentrations to the total amount initially present in the saltstone sample.

In addition to the effluent constituent discussed above, an extensive list of chemical parameters (i.e., alkalinity, DO, NO_3^-, NO_2^-, PO_4^{3-}, S^{2-}, SO_4^{2-}, Al, Ca, Fe, Mg, Mn, Na, $S_{total,}$ Si, etc.) will be monitored to provide a more comprehensive data set that can be used to better understand the relevant reactions occurring within the intact saltstone. A fourth test cell containing another ^{99}Tc-spiked test sample is currently being saturated to provide a fourth test treatment at another flow rate. To date only the first effluent sample has been collected with much of the analysis still ongoing. However, the effluent ^{99}Tc levels were actually quite low, ranging from 186 to 403 pCi mL^{-1}, with pH values that were ≥12.7. The initial data is plotted on Figure 10 for comparison with other intact saltstone leachate data sets discussed above, with the ^{99}Tc level appearing quite low for the high initial pH, although the pH is consistent with initial stages of cement weathering described by Ochs at al. (2016).

5.0 Discussion

The current report includes additional data from a series of EPA Method 1315 leaching tests conducted on monolithic saltstone samples collected from SDU Cell 2A and continued testing and refinement to the DLM procedure. The EPA 1315 leaching data for ^{129}I from the SDU Cell 2A samples indicated retention within the saltstone when compared to ^{137}Cs, and ^{99}Tc results for the same tests. A set of ^{129}I spiked saltstone simulants based on several different SDU grout formulations for use in future DLM tests are currently curing. The updated DLM results for the two SDU Cell 2A saltstone samples and the ^{99}Tc-spiked saltstone simulant provide a unique data set that is difficult to interpret because of variations in the flow rate between the three tests samples and changes in flow rate over time for a given sample, an inherent limitation of the system where inlet pressure was used to drive flow. To address this limitation, the DLM system was modified such that inlet flow rates can be maintained using micro-flow pumps that can withstand the required backpressure. In addition, an in-line septa-based system was developed so that effluent samples can be collected from the outlet tubing using a needle and syringe such that pH, ORP, and even DO measurements can be made on saltstone effluent before exposure to the atmosphere. The pH and ORP values collected using this method were generally consistent with expectations for cement pore waters during the initial stages of weathering.

6.0 Acknowledgements

The author would like to acknowledge the assistance of J. Cochran, K. Price, and C. Fulghum with completion of the laboratory studies and production of this report.

7.0 References

Almond, P.M., D.I. Kaplan, C.A. Langton, D.B. Stefanko, W.A. Spencer, A. Hatfield, and Y. Arai (2012) Method Evaluation and Field Sample Measurements for the Rate of Movement of the Oxidation Front in Saltstone. SRNL, Aiken, SC 29808.

APHA (1997) Method-4500-Nitrogen. Standard Methods for the Examination of Water and Wastewater, Washington, DC 20005.

ASTM (1999) Standard Practice for Microwave Digestion of Industrial Furnace Feedstreams and Waste for Trace Element Analysis. West Conshohocken, PA 19428-2959.

ASTM (2016) ASTM D7168-16: Standard Test Method for ^{99}Tc in Water by Solid Phase Extraction Disk, West Conshohocken, PA 19428-2959.

ASTM (2013) ASTM D7283-13 Standard Test Method for Alpha and Beta Activity in Water by Liquid Scintillation, West Conshohocken, PA 19428-2959.

ASTM (2008) ASTM D6527: Test Method for Determining Unsaturated and Saturated Hydraulic Conductivity in Porous Media by Steady-State Centrifugation, West Conshohocken, PA 19428-2959.

ASTM (2010) ASTM D5084-10: Standard Test Methods for Measurement of Hydraulic Conductivity of Saturated Porous Materials Using a Flexible Wall Permeameter, ASTM International, West Conshohocken, PA 19428-2959.

ASTM (2006) ASTM D2434 – 68: Standard Test Method for Permeability of Granular Soils (Constant Head), ASTM International, West Conshohocken, PA 19428-2959.

Bannochie C.J. (2012) Results of the Third Quarter 2012 Tank 50 WAC Slurry Sample: Chemical and Radionuclide Contaminants, Savannah River National Laboratory, Aiken, SC 29808. SRNL-STI-2012-00621.

Bannochie, C. J. (2014). "Results of the Third Quarter 2013 Tank 50 WAC Slurry Sample : Chemical and Radionuclide Contaminants." Savannah River National Laboratory, Aiken, SC 29808.

Cantrell K.J., Williams B.D. (2013) Solubility control of technetium release from Saltstone by $TcO_2 \cdot xH_2O$. J. Nuclear Materials 437:424-431. DOI: http://dx.doi.org/10.1016/j.jnucmat.2013.02.049.

Cantrell K.J., Carroll K.C., Buck E.C., Neiner D., Geiszler K.N. (2013) Single-pass flow-through test elucidation of weathering behavior and evaluation of contaminant release models for Hanford tank residual radioactive waste. Applied Geochemistry 28:119-127.

Clesceri L.S., Greenberg A.E., Trussell R.R. (1989) Standard methods for the examination of water and wastewater American Public Health Association, Washington, DC.

Dickson J.O., Harsh J.B., Lukens W.W., Pierce E.M. (2015) Perrhenate incorporation into binary mixed sodalites: The role of anion size and implications for technetium-99 sequestration. Chemical Geology 395:138-143. DOI: http://dx.doi.org/10.1016/j.chemgeo.2014.12.009.

Dinwiddie, C., and Pickett, D. (2017). "Fiscal Year 2016 Saltstone Leaching Experiment—Status Report." Center for Nuclear Waste Regulatory Analyses.

El-Kamash, A.M., Sami, N.M., and El-Dessouky, M.I. (2011). Leaching Behavior of ^{137}Cs and ^{60}Co Radionuclides from Stabilized Waste Matrices. International Journal of Environmental Engineering Science 2, 199-211.

Garrabrants, A.C., F. Sanchez, C. Gervais, P. Moszkowicz, and D.S. Kosson (2002) The effect of storage in an inert atmosphere on the release of inorganic constituents during intermittent wetting of a cement-based material. Journal of Hazardous Materials 91:159-185.

Garrabrants A.C., Kosson D.S., DeLapp R., van der Sloot H.A. (2014) Effect of coal combustion fly ash use in concrete on the mass transport release of constituents of potential concern. Chemosphere 103:131-139. DOI: http://dx.doi.org/10.1016/j.chemosphere.2013.11.048.

Golovich, E.C., S.V. Mattigod, MMV Snyder, L. Powers, G.A. Whyatt, and D.M. Wellman. 2014. Radionuclide Migration through Sediment and Concrete: 16 Years of Investigations. PNNL-23841, Pacific Northwest National Laboratory, Richland, WA.

Harbour, J.P. and M.F. Williams (2010) Impact of Curing Temperature on the Saturated Liquid Permeability of Saltstone. Savannah River National Laboratory, Aiken, SC. SRNL-STI-2010-00745.

Icenhower J.P., Qafoku N.P., Zachara J.M., Martin W.J. (2010) The biogeochemistry of technetium: A review of the behavior of an artificial element in the natural environment. American Journal of Science 310:721-752.

Kabai E., Beyermann M., Seeger J., Savkin B.T., Stanglmaier S., Hiersche L. (2013) Separation technique for the determination of 99Tc in milk and dairy products in case of emergency. Applied Radiation and Isotopes 81:36-41. DOI: http://dx.doi.org/10.1016/j.apradiso.2013.03.031.

Langton CA. 2014. Technetium Oxidation in Slag-based Sodium Salt Waste Forms Exposed to Water and Moist Hanford Soil. SRNL-STI-2014-00399 Rev 0. Savannah River National Laboratory, Aiken, SC.

Langton C.A., Almond P.M. (2013) Cast stone oxidation front evaluation: Preliminary results for samples exposed to moist air, SRNL-STI-2013-00541.

Lehto J., Hou X. (2011) Chemistry and Analysis of Radionuclides Wiley-VCH, Weinheim, Germany.

Lukens W.W., Bucher J.J., Shuh D.K., Edelstein N.M. (2005) Evolution of technetium speciation in reducing grout Environ. Sci. & Technol. 39:8064-8070.

Lukens W.W., McKeown D.A., Buechele A.C., Muller I.S., Shuh D.K., Pegg I.L. (2007) Dissimilar Behavior of Technetium and Rhenium in Borosilicate Waste Glass as Determined by X-ray Absorption Spectroscopy. Chemistry of Materials 19:559-566. DOI: 10.1021/cm0622001.

Lee W., Batchelor, B. (2003) Reductive capacity of natural reductants. Environ. Sci. Technol. 37:535-541.

Maset E.R., Sidhu S.H., Fisher A., Heydon A., Worsfold P.J., Cartwright A.J., Keith-Roach M.J. (2006) Effect of Organic Co-Contaminants on Technetium and Rhenium Speciation and Solubility under Reducing Conditions. Environmental Science & Technology 40:5472-5477. DOI: 10.1021/es061157f.

Mattigod, S. V., Westik, J. H., Chung, C. W., Lindberg, M. J., and Parker, K. E. (2011). "Waste Acceptance Testing of Secondary Waste Forms: Cast Stone, Ceramicrete and DuraLith." Pacific Noerthwaest National Laboratories. PNNL-20632.

McCloy J.S., Riley B.J., Goel A., Liezers M., Schweiger M.J., Rodriguez C.P., Hrma P., Kim D.S., Lukens W.W., Kruger A.A. (2012) Rhenium Solubility in borosilicate nuclear waste glass: Implications for the processing and immobilization of technetium-99. Environ. Sci. & Technol. 46:12616-12622.

Neeway J.J., N. Qafoku, R.J. Serne, A.R. Lawter, J.R. Stephenson, W.W. Lukens, and J.H. Westsik, Jr. (2014) Evaluation of Technetium Getters to Improve the Performance of Cast Stone. PNNL-23667, Pacific Northwest National Laboratory, Richland, WA.

Ochs, M., Mallants, D., and Wang, L. (2016). "Radionuclide and Metal Sorption on Cement and Concrete," Springer, New York.

Perkin Elmer Field Application Report, The Determination of Iodine in Food with the ELAN DRC-e ICP-MS (http://www.perkinelmer.com/Content/applicationnotes/far_iodineinfoodwithelandrc-e.pdf).

Pierce E.M., Lukens W.W., Fitts J.P., Jantzen C.M., Tang G. (2014) Experimental determination of the speciation, partitioning, and release of perrhenate as a chemical surrogate for pertechnetate from a sodalite-bearing multiphase ceramic waste form. Applied Geochemistry 42:47-59. DOI: http://dx.doi.org/10.1016/j.apgeochem.2013.12.017.

Roberts, K.A., and D.I. Kaplan (2009) Reduction Capacity of Saltstone and Saltstone Components. Savannah River National Laboratory, Aiken, SC, SRNL-STI-2009-00637.

Sayed, M. S., and Khattab, M. M. (2010). Immobilization of Liquid Radioactive Wastes by Hardened Blended Cement - White Sand Pastes. J. American Science 6, 334-341.

Serne R.J., J.H. Westsik Jr., Williams B.D., Jung H.B., Wang G. (2015) Extended Leach Testing of Simulated LAW Cast Stone Monoliths, Pacific Northwest National Laboratory, PNNL-24297 RPT-SLAW-001 Rev 0, Richland,

Seaman J.C., H.S. Chang, and S Buettner. (2014) Chemical and Physical Properties of Saltstone as Impacted by Curing Duration, SREL Doc. R-14-0006, ver. 1.0. Submitted to SRR September 23, 2014.

Seaman, J.C., H.S. Chang, and S.W. Buettner. 2013. Comparison of Hydraulic Property Measurement Techniques for Simulated Saltstone. SREL Doc. R-13-0006, ver. 1.0. Submitted to SRR September 4, 2013.

Shu X., Shen L., Wei Y., Hua D. (2015) Synthesis of surface ion-imprinted magnetic microsphere for efficient sorption of perrhenate: A structural surrogate for pertechnetate. Journal of Molecular Liquids 211:621-627. DOI: http://dx.doi.org/10.1016/j.molliq.2015.07.059.

Simner, S. P. (2016). Property Data for Core Samples Extracted from SDU Cell 2A. Savannah River Remediation. SRR-CWDA-2016-00051.

Strom R.N., Kaback D.S. (1992) SRP Baseline Hydrogeologic Investigation: Aquifer Characterization Groundwater Geochemistry of the Savannah River Site and Vicinity (U), Westinghouse Savannah River Company, Environmental Sciences Section, Aiken, SC. pp. 98.

Stumm W., Morgan J.J. (1995) Aquatic chemistry: An introduction emphasizing chemical equilibria in natural waters. 3rd ed. Wiley-Interscience, New York.

USEPA. (1992) Method 1311: Toxicity Characteristic Leaching Procedure, Test Methods for Evaluating Solid Waste, Physical/Chemical Methods (SW-846), Office of Solid Waste, Washington, DC.

USEPA (1996) Method 3052, Rev. 0 Microwave assisted acid digestion of siliceous and organically based matrices. Test Methods for Evaluating Solid Waste, Physical/Chemical Methods (SW-846), Office of Solid Waste, Washington, DC.

USEPA (2007) Method 6020A, Rev. 1. Inductively coupled plasma-mass spectrometry, Test Methods for Evaluating Solid Waste, Physical/Chemical Methods (SW-846), Office of Solid Waste, Washington, DC.

USEPA (2013) Method 1315, Mass transfer rates of constituents in monolithic or compacted granular materials using a semi-dynamic tank leaching procedure. Test Methods for Evaluating Solid Waste, Physical/Chemical Methods (SW-846), Office of Solid Waste, Washington, DC.

Westsik J.H., Jr, G.F. Piepel, M.J. Lindberg, P.G. Heasler, T.M. Mercier, RL Russell, A. Cozzi, W.E. Daniel Jr, R.E. Eibling, E.K. Hansen, M.M. Reigel, and D.J. Swanberg. 2013. Supplemental Immobilization of Hanford Low-Activity Waste: Cast Stone Screening Tests. PNNL-22747, Pacific Northwest National Laboratory, Richland, WA.

8.0 Appendix A1: Data Summary for EPA Method 1315

Monolith Sample Designation:		SDU-A = SDU2A-0931-C-1-U-2			
BFS Source:				Holcim	
Curing Duration:				20+ Months	
Sample Volume (mL):				1514	
Sample No.	Days	pH	^{99}Tc (pCi mL^{-1})	137Cs (pCi mL^{-1})	^{129}I (pCi L^{-1})
1	0.08	ND	0.76	348	7.11
2	1	11.24	1.65	655	20.2
3	2	11.11	1.44	495	13.1
4	7	11.37	4.02	1112	33.0
5	15.3	11.44	3.75	980	27.9
6	28	11.40	3.81	1080	29.4
7	42	11.41	3.71	984	25.0
8	49	11.10	2.33	701	13.5
9	63	11.19	2.82	778	14.4
Monolith Sample Designation:		SDU-B = SDU2A-0931-C-1-U-5			
BFS Source:				Holcim	
Curing Duration:				20+ Months	
Sample Volume (mL):				1514	
Sample No.	Days	pH	^{99}Tc (pCi mL^{-1})	137Cs (pCi mL^{-1})	^{129}I (pCi L^{-1})
1	0.08	ND	0.48	207	4.00
2	1	11.24	1.28	326	12.9
3	2	11.10	1.51	259	6.14
4	7	11.37	4.02	563	15.2
5	15.3	11.45	3.66	479	11.5
6	28.0	11.40	4.12	523	14.3
7	42.0	11.45	3.62	488	13.9
8	49.0	11.10	2.13	350	6.08
9	63	11.21	2.80	383	10.60
Monolith Sample Designation:		SDU-C = SDU2A-0931-C-2-U-2			
BFS Source:				Holcim	
Curing Duration:				20+ Months	
Sample Volume (mL):				1872	
Sample No.	Days	pH	^{99}Tc (pCi mL^{-1})	137Cs (pCi mL^{-1})	^{129}I (pCi L^{-1})
1	0.08	11.13	0.55	334	9.66
2	1	11.36	2.36	558	15.8
3	2	11.00	1.57	358	9.03
4	7	11.46	4.01	734	20.7
5	14	ND	3.44	608	16.5
6	28	11.42	4.17	693	23.5
7	42	11.35	2.82	435	16.3
8	49	11.13	0.88	212	5.99
9	63	11.10	2.51	314	11.7
ND = Not determined					